Inaccessible Porosity in Gasification Reactions under Kinetic Control

Evangelos A. Delikouras and Daniel D. Perlmutter
Dept. of Chemical Engineering, University of Pennsylvania, Philadelphia, PA 19104

Random pore models have been successful in interpreting a wide range of experimental observations in gas-solid reactions; however, their applicability has been limited to cases where the entire porous structure is initially accessible to reacting gases. In many practical cases, porous solids contain significant void regions that are initially inaccessible to gaseous reactants, but become accessible in the course of the reaction. A conceptual and mathematical model is developed here that accounts for the existence of this hidden porosity. It uses the same representation of the porous network as was developed in the earlier random pore models, but introduces physically meaningful expressions for the discovery of hidden pores, and the subsequent growth of the discovered pores. The modified model calls for only one additional parameter, the initial volume fraction of hidden porosity in the total volume. It is demonstrated computationally that neglecting hidden porosity can lead to serious underestimations of conversion and reaction rates.

Introduction

It was recognized at least as early as 1962 (Kawahata and Walker) that the reaction of porous solids with fluid reactants can be affected by the existence of void space that is not accessible to the fluid reactants. This void space can be inherent in the solid material, or it can be introduced secondarily in the course of a preparatory step, such as pelletizing or sintering. It is variously referred to as closed, inaccessible or isolated pore volume. These names, however, can be misleading, because they fail to indicate that these pores can become progressively accessible as reaction proceeds. With this in mind, it might be preferable to describe these enclosed pores as hidden.

Lacan (1972) uses a very informative comparison to summarize the basic ideas that underlie this model development: "... nothing, however deep in the bowels of the earth a hand may seek to ensconce it, will ever be hidden there, since another hand can always retrieve it, and that what is hidden is never but what *is missing from its place*, as the call slip puts it when speaking of a volume lost in a library. And even if the book be on an adjacent shelf or in the next slot, it would be hidden there, however visibly it may appear." This analogy is pertinent especially when one recalls that the measurement of pore volumes or surface areas depends almost always on pore filling or physical adsorption by mercury, nitrogen, carbon dioxide, or other inert gas. Pores in certain size ranges or with certain shapes may be hidden from one gas, while visible to others, just as the book on Lacan's adjacent shelf is hidden only in a limited sense.

The grain model of Szekely and Evans (1970) and the pore models of Bhatia and Perlmutter (1980) and Gavalas (1980) for gas-solid reactions do not include the existence of hidden pores in their conceptual framework. The work of Hashimoto and Silveston (1973), who used a population balance approach that allowed for initiation of new pores, could be considered as an attempt to account for hidden porosity; however, because their approach included curve fitting with multiple adjustable parameters, it is not well suited for predictions based on initial physical conditions. In their discrete model, Zygourakis and Sandmann (1988) did take into account the existence of initially inaccessible pores, but only under strong intraparticle diffusional limitations.

While approaches based on percolation concepts (such as that of Mohanty et al., 1982) provide a natural framework for treating hidden or isolated pores, they leave unresolved the question of whether it is valid to use continuum reaction-diffusion equations near the percolation threshold. Reyes and Jensen (1986) made significant progress by using a bond percolation method to determine the influence of coordination

number on burn-off profiles. This result, however, is limited by the fact that the volume of isolated porosity cannot be changed independently, since it is tied to the specific choice of coordination number and initial accessible porosity.

The objective of this work is to quantify and explore the effect of hidden porosity on gasification reactions, by extending the conceptual basis of the random pore models developed by Bhatia and Perlmutter (1980) and Gavalas (1980) to include the existence of hidden pores, as well as their discovery and subsequent evolution.

Model Development

Consider the reaction of a porous solid A with a surrounding gas B that yields a gaseous product P, according to the stoichiometry:

$$A_{(s)} + bB_{(g)} \rightarrow P_{(g)} \tag{1}$$

The reaction takes place at the internal surface of the pores of the solid. It is assumed that the reaction is in the regime of kinetic control: the diffusion of the gases B and P to and from the reaction front is faster than the intrinsic rate of the reaction. Furthermore, the solid particle is considered isothermal.

The void space of the porous solid is represented by a population of randomly overlapping pores of size distribution $f(r)$, where $f(r)dr$ is the total length of pores that have size between r and $r+dr$, per unit of total volume. This population consists of pores that have access to the external surface of the solid and of those that are initially hidden from the surrounding gas. Let ϵ_0 and ζ_0 be the initial volumes of accessible and hidden pores, respectively, per unit of total volume. The remaining (nonporous solid) volume is referred to as skeletal solid. As the reaction proceeds, the surrounding reactant gas reacts with the solid. In so doing, it "gasifies" away the solid walls of the accessible pores, discovering in the process the hidden pores. A hidden pore is discovered the moment it coalesces with a currently accessible pore, regardless of whether this pore was originally accessible or hidden. Let V_D be the cumulative volume discovered up to time t, with V_H the remaining hidden volume. Thus,

$$\zeta_0 = V_D + V_H \tag{2}$$

Once a hidden pore is discovered, it starts growing with the same kinetics as one that was originally accessible. Let V_G be the growth of pore volume that is directly attributable to the reaction of the discovered volume, that is, to the once-hidden volume that has become accessible by time t. In contrast, let V_E be the growth that has occurred over the time interval from 0 to t that started from the initially accessible pores. Note that the discovered volume is entirely within and a part of either V_E or V_G, because a hidden pore can only be discovered via growth over time of either an initially accessible pore or a discovered pore. Using these definitions, the fraction of the overall volume that is occupied by void space at any time is:

$$V_T = \epsilon_0 + V_E + V_G + V_H \tag{3}$$

Conversion X is defined as usual as the fraction of the *available* solid that has reacted. In the presence of hidden porosity, however, it should be noted that the fractional volume of solid available for reaction is not $(1-\epsilon_0)$, but rather $(1-\epsilon_0-\zeta_0)$. Thus,

$$X = \frac{V_T - \epsilon_0 - \zeta_0}{1 - \epsilon_0 - \zeta_0} \tag{4}$$

which, by using Eqs. 2 and 3, becomes:

$$X = \frac{V_E + V_G - V_D}{1 - \epsilon_0 - \zeta_0} \tag{5}$$

Equation 5 carries the important message that while the growth of the discovered pores contributes to the conversion of the solid, the mere *discovery* of those pores does not *per se* contribute to conversion.

To determine the actual pore volume of the solid, one must account for the random intersections among neighboring growing pores. Avrami's relationship (Avrami, 1940) provides the link between overlapping pores and the corresponding nonoverlapping pores.

$$V_T = 1 - \exp(-V_{TX}) \tag{6}$$

where V_{Tx} denotes the nonoverlapping total void volume. By incorporating Eq. 6 into the definition of conversion and rearranging one obtains:

$$\begin{aligned} X &= 1 - \frac{1 - V_T}{1 - \epsilon_0 - \zeta_0} \\ &= 1 - \frac{\exp(-V_{Tx})}{1 - \epsilon_0 - \zeta_0} \\ &= 1 - \frac{\exp[-\epsilon_{0x} - V_{Ex} - V_{Gx} - (\zeta_{0x} - V_{Dx})]}{1 - \epsilon_0 - \zeta_0} \end{aligned} \tag{7}$$

Evaluation of Eq. 7 requires, in addition to the knowledge of V_{Ex}, that particulars be available on the hidden porosity that has been discovered as well as the extent of its growth. For this purpose, it may be taken that the discovery rate of hidden pores equals the rate at which total accessible porosity grows as the solid retreats, multiplied by the fractional expectation p that such growth will uncover a hidden pore. Then,

$$\frac{dV_{Dx}}{dt} = p\left(\frac{dV_{Ex}}{dt} + \frac{dV_{Gx}}{dt}\right) \tag{8}$$

where in the beginning of the reaction:

$$V_{Dx}(0) = 0 \tag{9}$$

The expectation p of discovering a hidden pore is equal to the porous fraction of the apparent solid, that is, the ratio of remaining hidden porosity to the volume of solid that *appears* to remain unreacted:

$$p = \frac{V_H}{1 - \epsilon_0 - V_E - V_G} \tag{10}$$

Although the growth of the reaction surface of the discovered pores is governed by the same kinetics as that of the originally accessible surface, the volume growth rates are different, because the discovery of hidden pores is equivalent to length generation, whereas accessible surface grows without adding length. As shown by Bhatia and Perlmutter (1980), an analytical solution for the volume growth of the initially accessible pores is given by:

$$V_{Ex} = RS_{E0x}t + \frac{\pi R L_{E0x} t^2}{S_{E0x}} \tag{11}$$

where R is the rate of reaction interface movement, as determined by the kinetics of the reaction, and S_{E0x} and L_{E0x} are the initial internal surface area and length of the accessible pores, respectively. In contrast, the expression for volume evolution of the discovered pores must include a provision for the increase in total length, the link between the discovery and the subsequent growth of hidden pores. Assuming cylindrical geometry for the pores:

$$\frac{dV_{Gx}}{dt} = RS_{Gx} \tag{12}$$

$$\frac{dS_{Gx}}{dt} = 2\pi R L_{Gx} \tag{13}$$

with the initial conditions:

$$V_{Gx}(t=0) = S_{Gx}(t=0) = 0 \tag{14}$$

where S_{Gx} is the internal surface area of the discovered pores and L_{Gx} is the length of the discovered pores. If hidden pores are being discovered in a statistically representative way, it may be concluded that their length L_{Gx} at any instant t is the same fraction of its initial value as the discovered porosity is of the initial hidden porosity:

$$\frac{L_{Gx}}{L_{G0x}} = \frac{V_{Dx}}{\zeta_{0x}} \tag{15}$$

where L_{G0x} is the length of the hidden pores at the beginning of the reaction. In principle, length L_{G0x} could be measured directly if the initial pore size distribution function of the hidden pores were known. However, this distribution is extremely difficult to determine experimentally, at present at least. In cases where the distribution of hidden pores conforms to the rest of the porous structure, L_{G0x} is given by:

$$\frac{L_{G0x}}{L_{E0x}} = \frac{\zeta_{0x}}{\epsilon_{0x}} \tag{16}$$

By defining a dimensionless time $\tau = RS_{E0x}t$, the modeling equations become:

$$\frac{dV_{Dx}}{d\tau} = p\left(\frac{dV_{Ex}}{d\tau} + \frac{dV_{Gx}}{d\tau}\right) \tag{17}$$

$$\frac{dV_{Gx}}{d\tau} = \frac{S_{Gx}}{S_{E0x}} \tag{18}$$

$$\frac{dS_{Gx}}{d\tau} = \frac{2\pi}{S_{E0x}} \frac{V_{Dx}}{\epsilon_{0x}} L_{E0x} \tag{19}$$

with initial conditions:

$$V_{Dx}(\tau=0) = V_{Gx}(\tau=0) = S_{Gx}(\tau=0) = 0 \tag{20}$$

Equations 17 to 20 constitute a general description of the temporal evolution of the hidden porous structure of the reacting solid.

Numerical Results

The set of Eqs. 17 to 20 define the growth rates of interest, but do not provide a closed-form explicit solution. The system behavior, particularly the differences that arise from hidden porosity, must therefore be examined by numerical studies. To this end, consider a typical porous structure with $\epsilon_0 = 0.26$, $S_0 = 2.42 \times 10^3$ cm^2/cm^3, and $L_0 = 3.14 \times 10^6$ cm/cm^3, with a corresponding value of the structural parameter $\psi = 5$ (Bhatia and Perlmutter, 1980). For these choices of parameters, the system of differential equations (Eqs. 17–19), along with their initial conditions (Eq. 20), was integrated numerically by using a GEAR-type integrator. The time dependence of conversion was subsequently computed according to Eq. 7.

The results of the numerical study in Figures 1, 2 and 3 show how conversion and the conversion rate vary with time, and how the rate varies with conversion for various levels of hidden porosity between $\zeta_0 = 0$ and $\zeta_0 = 0.4$. In each case, the result for $\zeta_0 = 0$ is the important reference curve, since it represents the prediction of the prior random pore models (Bhatia and

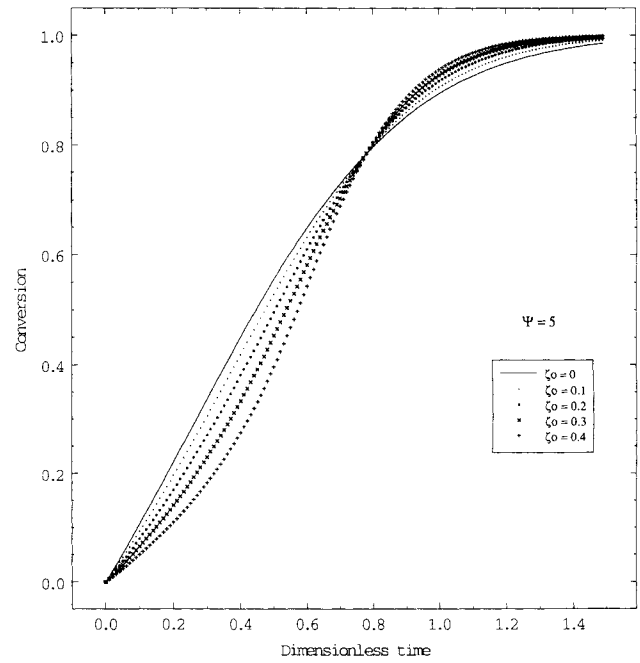

Figure 1. Conversion at different times for $\psi = 5$ at various levels of hidden porosity.

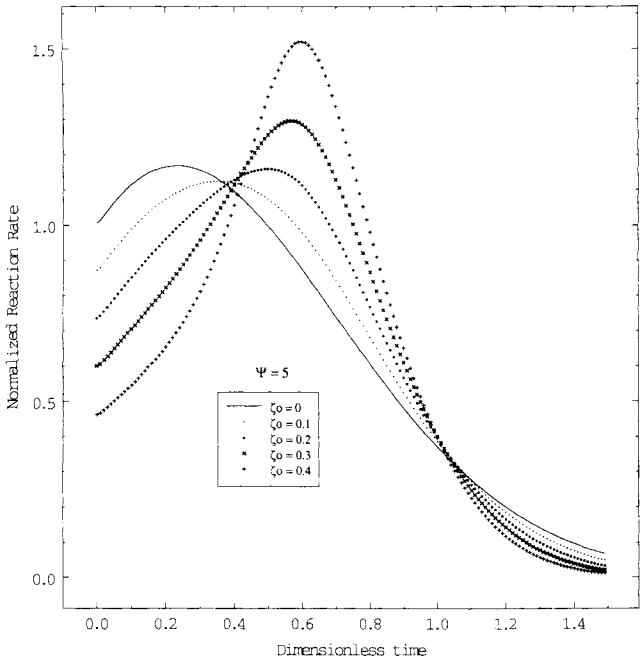

Figure 2. Gasification rates for $\psi = 5$ at various levels of hidden porosity.

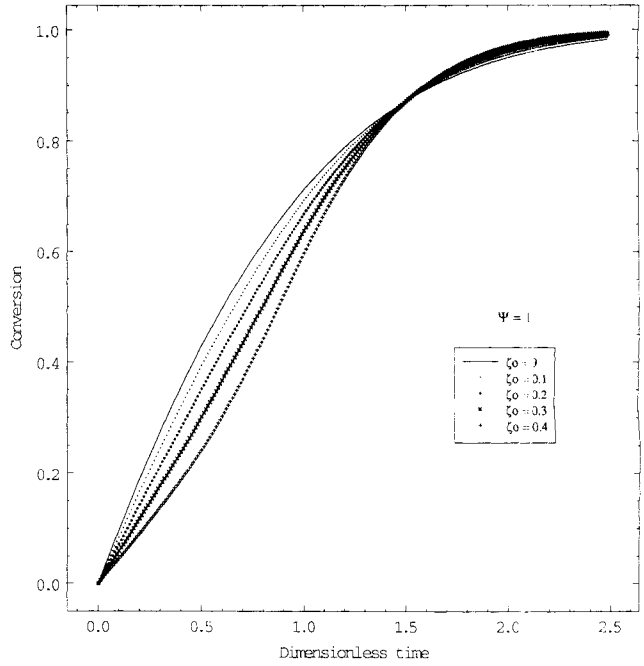

Figure 4. Conversion at different times for $\psi = 1$ at various levels of hidden porosity.

Perlmutter, 1980; Gavalas, 1980) that did not account for hidden porosity.

The results in Figure 1 show that in the initial stages of reaction conversion can be overestimated by as much as 17% if hidden pores are ignored. At longer times, conversion is underestimated, but by no more than 4.5%. Figure 2 shows the reaction rate vs. time behavior, in which a maximum in rate occurs for all levels of hidden porosity. This maximum is shifted to longer times compared to the prediction for no hidden porosity. For a sufficiently large value of hidden porosity $\zeta_0 \geq 0.3$, an inflection point also exists. An alternative way to present rate data is the so-called burn-off profile, which is given in Figure 3.

The effect of changes in the structural parameter on conversions and burn-off profiles is examined in Figures 4 through 7 by varying ψ, while holding the initial porosity at $\epsilon_0 = 0.26$

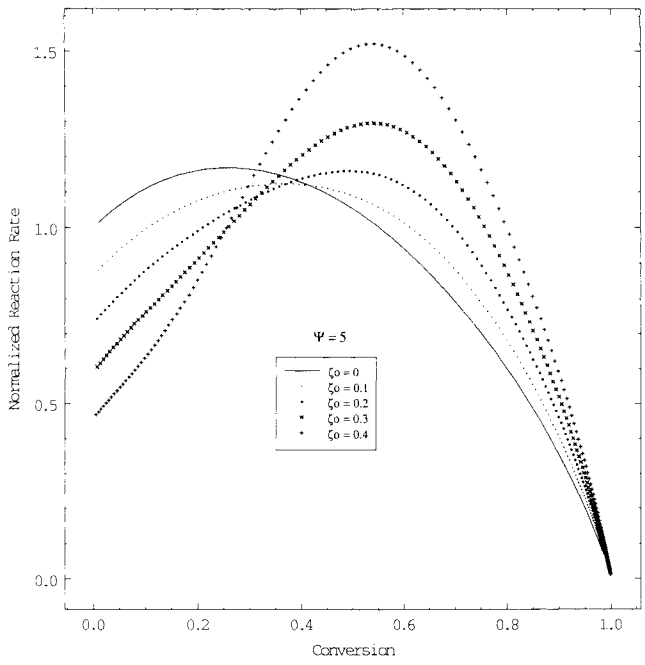

Figure 3. Burn-off profiles for $\psi = 5$ at various levels of hidden porosity.

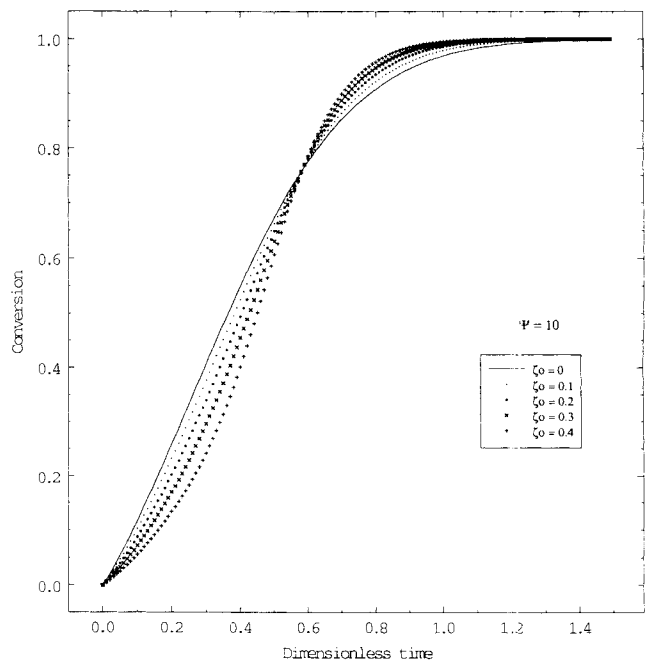

Figure 5. Conversion at different times for $\psi = 10$ at various levels of hidden porosity.

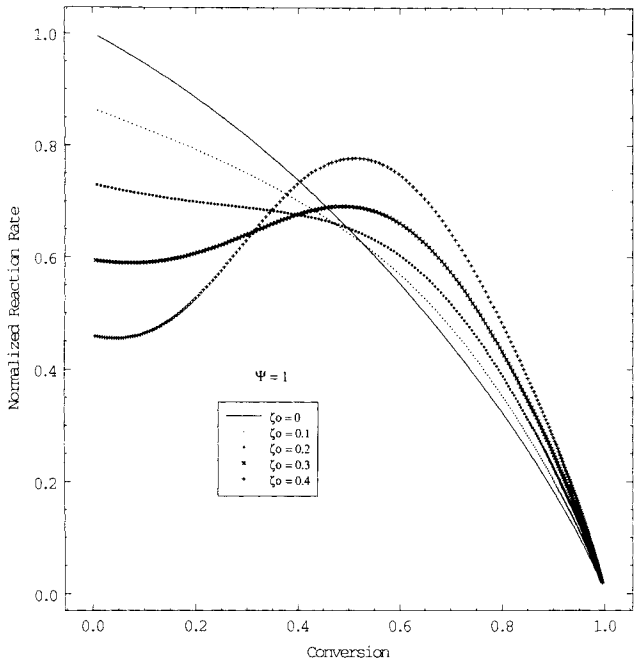

Figure 6. Burn-off profiles for $\psi = 1$ at various levels of hidden porosity.

as above. The surface areas and lengths of these comparisons are accordingly taken as follows:

$$S_0 = 12.1 \times 10^3 \text{ cm}^2/\text{cm}^3;\ L_0 = 15.7 \times 10^6 \text{ cm/cm}^3\ (\psi = 1)$$

and

$$S_0 = 1.21 \times 10^3 \text{ cm}^2/\text{cm}^3;\ L_0 = 1.57 \times 10^6 \text{ cm/cm}^3\ (\psi = 10).$$

The conversions for $\psi = 1$ are found to be much slower than those for $\psi = 5$, and they are again overestimated in the beginning of the reaction by as much as 20%. Near the end of the reaction, the underestimations are only about 1.5%. The corresponding values for the choice of $\psi = 10$ are 14% and 5%, respectively. The burn-off profiles in Figures 6 and 7 show that at the higher parameter value of $\psi = 10$, there always exists a maximum in rate as there was for $\psi = 5$. In contrast, for the lower value $\psi = 1$, a maximum occurs only for $\zeta_0 = 0.3$ and $\zeta_0 = 0.4$, and the rate monotonically decreases for the smaller values of $\zeta_0 = 0.1$ and $\zeta_0 = 0.2$.

Discussion

To explain the effect of hidden porosity on the conversion curves, one should look into the relative magnitudes of the discovered porosity and the growth of discovered porosity. Typical results are presented in Figure 8 for the choice of $\psi = 5$ and $\zeta_0 = 0.1$, demonstrating that reaction due to discovered porosity initially lags behind the discovery of hidden porosity. In other words, in the early stages of the reaction discovered porosity does not have sufficient time to grow significantly and delays conversion. That is why conversion is initially overestimated by random pore models that neglect hidden pores. This picture is soon altered: a reversal occurs when the discovery of hidden porosity comes to an end, while the growth of the discovered pores proceeds apace. In this sense, discovered porosity is initially a liability, since it contributes nothing to conversion, but this liability turns into an asset as it progressively makes more surface area available to reaction.

Examining the burn-off profiles in Figures 3, 6 and 7, it is clear that the position of the maximum rate on the conversion scale is very sensitive to the level of hidden porosity. Bhatia and Perlmutter (1980) showed that for $\zeta_0 = 0$, a reaction rate maximum can be expected only for $\psi > 2$ and that this maximum occurs at the conversion level:

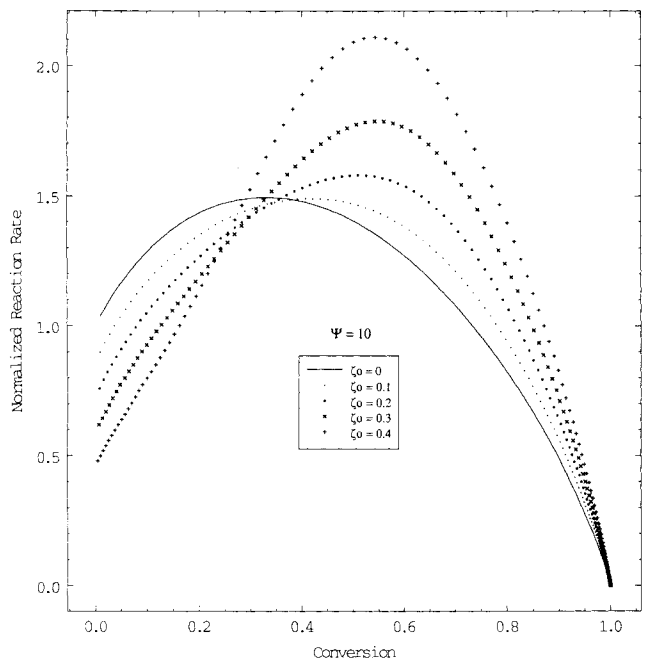

Figure 7. Burn-off profiles for $\psi = 10$ at various levels of hidden porosity.

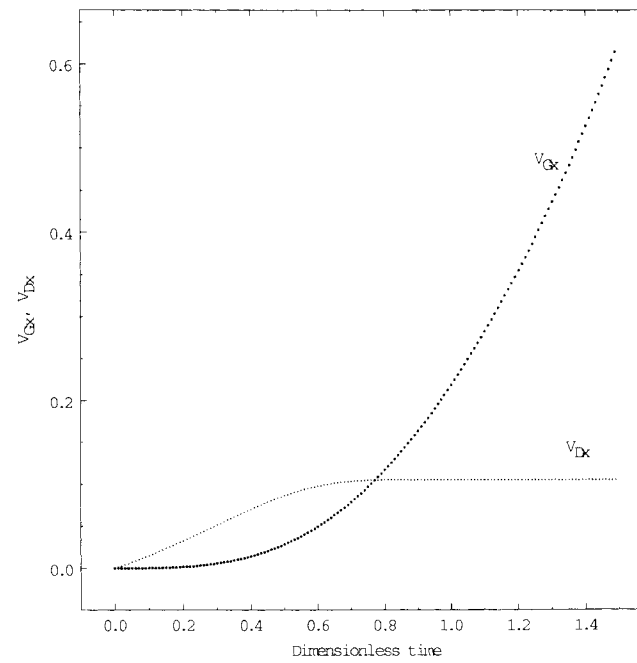

Figure 8. Discovered porosity and its subsequent growth as a function of time ($\psi = 5$ and $\zeta_0 = 0.1$).

$$X_M = 1 - \exp\left(\frac{2-\psi}{2\psi}\right) \tag{21}$$

with:

$$0 < X_M < 0.393 \tag{22}$$

It should be emphasized that since Eq. 21 does not permit any $X_M > 0.393$, data that exceed this limit cannot be interpreted by the simpler model. Examples may be found in the work of Kawahata and Walker (1962), where rate maxima are reported at conversions in the range between $X = 0.40$ and $X = 0.50$. In the new model where hidden porosity is accounted for, there is no simple analytical way to determine the minimum ψ value for which a rate maximum exists, but from the numerical example with $\psi = 1$, it is clear that the existence of a maximum also depends on the amount of hidden porosity. Although no maximum would have been expected according to the earlier random pore models (since $\psi < 2$), a maximum does, in fact, appear up to $\zeta_0 > 0.2$. For $\zeta_0 = 0.3$, a shallow maximum exists, and for $\zeta_0 = 0.4$, a much more pronounced maximum appears. For $\psi = 5$, a maximum always exists, as expected; however, this maximum is always shifted toward higher conversions up to $X_M = 0.53$, whereas Eq. 21 for $\zeta_0 = 0$ would have predicted a limit of $X_M = 0.258$.

Conclusions

In essence, the model presented here for gasification of porous solids under kinetically controlled conditions quantifies the competition among pore growth, pore coalescence, and discovery of hidden pores. The numerical results demonstrate that hidden porosity can be responsible for substantial departures from expected behaviors with respect to both conversions and reaction rates. The model reduces to an earlier random pore model in the limiting case of no hidden porosity. This ancestor model required only input information about the initial pore structure in the form of the structural parameter ψ. The modified model introduced here calls only for one additional parameter ζ_0, preferably to be determined by physical measurements before the chemical reaction begins, but alternatively to be estimated in the process of kinetic data interpretation. The modified model broadens the subset of experimental observations that can be interpreted and can also be instrumental in the design of gasifiers for materials with significant content of hidden porosity. Finally, it provides the necessary concepts and tools for further exploring the effect of hidden porosity in various solids.

Notation

L_E = length of initially accessible pores
L_G = length of discovered pores
R = rate of movement of reaction interface
S_E = surface area of initially accessible pores
S_G = surface area of discovered pores
V_E = volume growth of initially accessible porosity
V_G = volume growth of discovered porosity
V_D = volume of discovered porosity
V_H = volume of hidden porosity
V_T = volume of total porosity
X = conversion
t = time

Greek letters

ϵ_0 = initially accessible porosity
ζ_0 = initially inaccessible or hidden or isolated porosity
ψ = structural parameter of the solid = $4\pi L_{E0x}/S_{E0x}^2$
τ = dimensionless time = $RS_{E0x}t$

Subscripts

x = nonoverlapped quantities
0 = initial quantities

Literature Cited

Avrami, M., "Kinetics of Phase Change: II. Transformation-Time Relations for Random Distribution of Nuclei," *J. Chem. Phys.*, **8**, 212 (1940).

Bhatia, S. K., and D. D. Perlmutter, "A Random-Pore Model for Fluid-Solid Reactions: I. Isothermal, Kinetic Control," *AIChE J.*, **26**, 379 (1980).

Gavalas, G. R., "A Random Capillary Model with Application to Char Gasification at Chemically Controlled Rates," *AIChE J.*, **26**, 577 (1980).

Hashimoto, K., and P. L. Silveston, "Gasification: I. Isothermal, Kinetic Control Model for a Solid with a Pore Size Distribution," *AIChE J.*, **19**, 259 (1973).

Kawahata, M., and P. L. Walker, "Mode of Porosity Development in Activated Anthracite," *Proc. Carbon Conf.*, **2**, 251, Pergamon Press (1962).

Lacan, Jacques, "Seminar on the 'The Purloined Letter,'" *Freud: Structural Studies in Psychoanalysis*, in French, Yale French Studies, **48**, 39 (1972); Muller, J. P., and W. J. Richardson, eds., *The Purloined Poe*, p. 40, Johns Hopkins Univ. Press, Baltimore (1988).

Mohanty, K. K., J. M. Ottino, and H. T. Davis, "Reaction and Transport in Disordered Media: Introduction of Percolation Concepts," *Chem. Eng. Sci.*, **37**, 905 (1982).

Reyes, S., and K. F. Jensen, "Percolation Concepts in Modelling of Gas-Solid Reactions: I. Application to Char Gasification in the Kinetic Regime," *Chem. Eng. Sci.*, **41**, 333 (1986).

Szekely, J., and J. W. Evans, "A Structural Model for Gas-Solid Reactions with a Moving Boundary," *Chem. Eng. Sci.*, **25**, 1091 (1970).

Zygourakis, K., and C. W. Sandman, Jr., "Discrete Structural Models and Their Application to Gas-Solid Reacting Systems," *AIChE J.*, **34**, 2030 (1988).

Manuscript received July 26, 1991.